Exfoliation and Spray Deposition of Graphene Nanoplatelets in Ethyl Acetate and Acetone: Implications for Additive Manufacturing of Low-Cost Electrodes and Heat Sinks

Muhammed Ramazan Oduncu,[1] Zhifan Ke,[2] Bingyuan Zhao,[1] Zhongxia Shang,[1] Robin Simpson,[3] Haiyan Wang,[1] Alexander Wei[1,2,*]

[1] School of Materials Engineering, Purdue University, 701 West Stadium Avenue, West Lafayette, IN 47907 USA

[2] Department of Chemistry, Purdue University, 560 Oval Drive, West Lafayette, IN 47907 USA

[3] Thermo Fisher Scientific, East Hampshire GU32 3DL, United Kingdom

* Corresponding author. E-mail: alexwei@purdue.edu

ABSTRACT

Nonaqueous dispersions of graphene nanoplatelets (GrNPs) can be used to prepare thin films and coatings free of surfactants, but typically involve polar organic solvents with high boiling points and low exposure limits. Here we describe the mechanochemical exfoliation and dispersion of GrNPs in volatile aprotic solvents such as ethyl acetate (EtOAc) and acetone, which rank favorably in green solvent selection guides. GrNPs in powder form were exfoliated with solvent on a horizontal ball mill for 48 hours then sonicated at moderate power, to produce suspensions in excess of 300 μg/mL with minimum loss of dispersion stability over 7 weeks at room temperature. Atomic force microscopy (AFM) of individual particles indicate a median thickness and lateral width of 8–10 layers and 180 nm, respectively. GrNP films can be deposited by conventional airbrush equipment with a dry time of seconds and applied as layers and coatings that enhance the reproducibility and performance of electronic devices. We demonstrate the utility of spray-coated GrNPs as contact layers for low-cost electrochemical sensing with improvements in intrabatch reproducibility, and as conformal coatings on metal heat sinks with enhanced rates of heat dissipation.

KEYWORDS: graphene, liquid-phase exfoliation, electrochemical sensors, heat exchange, nanomanufacturing

INTRODUCTION

Graphene, the quintessential two-dimensional crystalline material, was initially characterized as such by Geim and Novoselov in 2004.[1] The reduced dimensionality of graphene gives rise to a variety of exciting physical properties, many of which are tunable as a function of layer number between 1 and 10.[2,3] The electronic properties of few-layered graphene has attracted much interest as a processible material for applications in flexible hybrid electronics,[4] energy storage,[5] smart coatings,[6] and sensors.[7] The integration of graphene-enhanced materials into thin-film technologies can be advanced by practical and scalable methods for depositing graphene under conditions that are cost-effective, while maintaining high levels of device performance and reproducibility.

Graphene interfaces can be prepared by top-down deposition or bottom-up chemical growth.[2] The former approach is more versatile and economical than the latter, which is energy-intensive or involves catalytically active substrates. From a manufacturing perspective, liquid-phase deposition of graphene is scalable but depends on methods that can produce stable dispersions of high-quality, few-layer graphene in acceptable processing solvents.[8,9] Graphite that is exfoliated oxidatively then reduced (rGO) typically have more defects than other sources of graphene,[10,11] which can affect applications that rely on electronic stability. Higher quality graphene can be prepared by electrochemical exfoliation but involves auxiliary electrolytes and polar organic solvents.[12] Mechanochemical exfoliation is the simplest and most appropriate method for producing graphene dispersions, with water or aqueous mixtures being the favored medium.[9,13,14,15,16] However, the use of protic solvents requires surfactants or charge-modified graphene for dispersion stability, which can interfere with the performance and reproducibility of electronic properties.[17,18]

Mechanochemical exfoliation of high-quality graphene without surfactants can be achieved using aprotic organic solvents.[9,19,20,21] *N*-methyl-2-pyrrolidone (NMP), *N,N*-dimethylformamide (DMF), and *o*-dichlorobenzene (ODCB) are the most commonly used, but have low volatility (bp >150 °C) and are difficult to remove by standard drying methods. All three are deemed hazardous to human health with permissible exposure limits (PEL) of 1, 10, and 50 ppm, respectively.[22,23] DMF and NMP are reprotoxic and rank in the lowest tier of multiple selection guides for sustainable solvents,[24,25,26] and are on the REACH candidate list of substances of very high concern (SVHP).[27] Although less is known about ODCB, it is a high-priority substance for risk evaluation by the U.S. Environmental Protection Agency (EPA).[28]

There have been numerous attempts to disperse graphene in organic solvents with higher volatility and/or lower toxicity. Coleman and coworkers performed a systematic analysis on the dispersion stability of graphene in various organic solvents with low surface tension ($\leq$40 mJ/m^2) in the context of Hansen and Hildebrandt solubility parameters, with δ_D values in the range of 15–21 MPa$^{0.5}$ being the most relevant.[29] Although their study implies that graphene can form stable dispersions in a wide range of solvents, very few practical advances have been made. The stability limit of most surfactant-free dispersions after centrifugation is below 10 μg/mL,[9,29] although densities up to 500 μg/mL have been reported with chloroform and isopropanol, and up to 80 μg/mL with acetone.[30]

The lateral dimension of graphene is a parameter that can affect dispersion stability in organic solvents, but one that has not been examined deeply. Graphene exfoliated from bulk sources of graphite typically have lateral size distributions on the order of microns;[9,19] However, graphene nanoplatelets (GrNPs) with submicron dimensions are also valuable for devices and interfaces that require very high surface-to-volume ratios. GrNPs are especially useful for

supporting transduction mechanisms between charge and electron mobility, such as electrical double-layer (EDL) capacitors[31] and contacts for solid-state ion-selective electrodes (ISEs).[32] Graphitic materials are also well known for their excellent heat conduction properties, with GrNPs having been used as fillers in composites for heat exchangers[33] and heat sinks,[34] and also as fluid suspensions for similar heat-transfer applications.[35] The spray-coating of GrNPs onto heat-exchange interfaces with large surface areas should thus be attractive from an additive manufacturing perspective, although such an application has yet to be reported.

To deposit GrNPs by conventional airspray methods, materials should be exfoliated in good processing solvents with low toxicity and high volatility for rapid drying times, preferably without surfactants that might hamper the ion-to-electron transduction properties of the GrNP interfaces. While the processing issues that face graphene still apply to GrNPs, the smaller size distribution of the latter may be sufficient to overcome some of the destabilizing forces that plague the dispersion of exfoliated graphene in most organic solvents.

Here we show that stable GrNP dispersions can be prepared by mechanochemical exfoliation in volatile, moderately polar aprotic solvents such as ethyl acetate (EtOAc) and acetone (Scheme 1), at concentrations above 350 μg/mL and yields by weight (Y_W) up to 62%. EtOAc and acetone have high PELs and rank favorably as green solvents (Table 1),[22–25] and their widespread use in paints, varnishes, and cosmetics supports their acceptable use as processing solvents for graphene dispersions and films. Both solvents have low surface tension and δ_D values within the range reported for stable graphene dispersions.[29] EtOAc ranks as a recommended (preferred) solvent in four out of five categories in the CHEM21 selection guide,[36] although its low flash point (–4 °C) makes its safety rating lower than that of alcohols. On the other hand, EtOAc can be prepared from biorenewable sources of ethanol and degrades into

nontoxic byproducts,[37] which further reduces its environmental impact. GrNP dispersions using either solvent are stable for many weeks and can be deposited across large areas by standard air-spray methods, with drying times on the order of seconds. We use GrNP spray coating to deposit solid contacts on screen-printed potentiometric electrodes for improved batch reproducibility, and conformal coatings on metal heat sinks for higher rates of heat dissipation.

Scheme 1. Graphene nanoplatelet (GrNP) powder can be exfoliated by low-energy ball milling to form stable dispersions in pristine EtOAc or acetone, enabling its deposition as thin films and conformal coatings with rapid drying using conventional airspray equipment.

Table 1. Characteristics of Select Organic Solvents for Graphene (Nanoplatelet) Dispersion

	EtOAc	**acetone**	**NMP**	**DMF**	**ODCB**
Surface tension (mJ/m^2)	23.75	25.20	40.8	37.1	36.6
Hansen parameters (MPa$^{1/2}$)					
Dispersion (δ_D)	15.8	15.5	18.0	17.4	19.2
Polarity (δ_P)	5.3	10.4	12.3	13.7	6.3
Hydrogen bond (δ_H)	7.7	7.0	7.2	11.3	3.3
Hildebrandt parameter (δ_T)	18.2	19.9	23.0	24.9	20.5
Boiling point (°C)	77	56	202	153	180
Vapor pressure (P_{vap}^0, torr)	93.2	230	0.34	3.9	1.4
PEL (ppm)[22,23]	400	1000	1.0	10	50
EHS indicator score[24,a]	2.9	3.1	--	3.7	--
GSK solvent guide[26,b]	16	15	7	7	--
Pfizer/Sanofi (CHEM21) solvent guides[24,36]	Recommend (preferred)	Recommend (problematic)	Substitute/ hazardous	Substitute/ hazardous	--

[a] Lower values indicate safer solvent. [b] Higher values indicate safer solvent.

EXPERIMENTAL SECTION

Materials. Graphene nanoplatelets prepared by thermal plasma treatment of methane was acquired in dry powder form from NanoIntegris/Raymor (PureWave^{TM}).[38] HPLC-grade ethyl acetate was used as received from Fisher Scientific and protected from air and moisture for up to four weeks. Reagent-grade acetone and anhydrous tetrahydrofuran (THF) were obtained from Fisher Scientific; acetone was dried with activated 3A molecular sieves prior to use. Cylindrical zirconia beads (1/4 × 1/4") were obtained from Glen Mills Inc.; spherical yttria-stabilized zirconia (YSZ) beads (5.5 mm) were obtained from MSE Supplies.

Liquid-assisted exfoliation was performed in 100-mL glass bottles (Pyrex) or 80-mL nylon jars (MTI Corp.) on a horizontal ball mill. Atomic force microscopy (AFM) and four-probe resistance measurements were performed using plasma-cleaned Si/SiO_2 substrates. Ion-selective electrodes were prepared using screen-printed carbon electrodes on polyethylene terephthalate (PET) roll substrates. Polyvinyl chloride (PVC; Selectophore grade, 150 kDa) and tetraoctylammonium bromide (TOAB, 98%), were obtained from Sigma–Aldrich; dibutyl phthalate (DBP, 99%) was obtained from Alfa–Aesar. Tetraoctylammonium nitrate (TOAN) was prepared from TOAB and sodium nitrate by ion-exchange chromatography.

Analytical instrumentation. Optical extinction spectra were obtained using a Cary-50 UV-Vis spectrophotometer (Varian). Transmission electron microscopy (TEM) images of graphene layers exfoliated using ZrO_2 or YSZ milling media were acquired using a Tecnai T20 (FEI) operating at 200 kV with a Gatan US1000 charge-coupled device camera. TEM analysis with selected-area electron diffraction (SAED) and energy-dispersive X-ray spectroscopy (EDS) was carried out with a FEI Talos 200X TEM operating at 200 kV with a high-angle annular dark field (HAADF) detector and SuperX EDS with four silicon drift detectors, and a 1.3-nm electron

probe for STEM imaging and EDS analyses. All SAED patterns were acquired using the same diffraction aperture. EDS composition maps were collected over a 15-min window using the drift correction mode. TEM samples were prepared by drop-casting dilute FLG dispersions onto holey carbon grids (400 mesh), allowing the solvent to evaporate in between drops.

Atomic force microscopy (AFM) analysis was performed in tapping mode using a Veeco Multi-Mode AFM with Nanoscope V controller, and a NanoSensors probe with a 125-μm cantilever operating at a resonance frequency of 330 kHz and a force constant of 42 N/m. Samples were prepared by drop-casting GrNP dispersions diluted 20-fold onto plasma-cleaned Si/SiO_2 substrates. X-ray photoelectron spectroscopy (XPS) and Raman spectroscopy were performed with a Thermo Scientific NEXSA surface analysis system. XPS data was acquired using a monochromatic Al Kα X-ray source (1486.7 eV) operating at 72 W. Survey and high-resolution XPS data was collected using spot sizes of 200 or 400 μm. Survey spectra were acquired at a pass energy of 200 eV, step size of 1 eV, dwell time of 50 ms, and energy range between −10 and 1350 eV. ~~High-resolution spectra were acquired for the C 1s, O 1s, and Si 2p regions using a pass energy of 50 eV, step size of 0.1 eV, and dwell time of 50 ms. The C KLL Auger region was investigated using a pass energy of 75 eV, step size of 0.5 eV, and dwell time of 1000 ms.~~ Raman spectra were acquired using the Thermo Scientific iXR module (integrated with the NEXSA) with a 532-nm excitation laser operating at a power of 10 mW and a 50-μm slit aperture. Raman and XPS analysis were performed on the same region of interest.

Sheet resistances of spray-coated GrNP layers were measured by the four-point probe method using a Keithley 4200 parameter analyzer. Au electrodes were sputtered onto graphene-coated Si/SiO_2 substrates using a lithographic mask, and current was applied under ambient

conditions through the two outer electrodes with potential differences (ΔV) measured between the two inner electrodes. Sheet resistance (R_S) and conductivity (σ) were calculated as

$$R_S(\Omega/sq) = \frac{\Delta V}{I} \times \frac{W}{L}$$

$$\sigma(S/cm) = 1/R_S \cdot t_{av}$$

with I, W, L, and t_{av} representing constant current, channel width and length, and mean film thickness as measured by AFM.

Potentiometric readouts were recorded with a National Instruments USB 6210 multi-channel analyzer supported by NI DAQ Express software; electrical noise was reduced by using shielded wires and installing 0.1-μF capacitors across each channel. A double-junction Ag/AgCl electrode (Orion 900200 Sure-Flow) with 1 M LiOAc outer filling solution was used as the reference. Heat dissipation studies were conducted with metal heat sinks bonded to the backs of thermoelectric plates powered by a 12-V rechargeable battery. Surface temperatures up to 90 °C were monitored using a thermographic IR imaging camera (FLIR SC305) with a reported sensitivity of 50 mK at 30°C and an accuracy of 2%.

Mechanochemical exfoliation and spray deposition. Ball milling was performed using a custom-made benchtop rolling mill operating at 350–400 rpm (Figure S1, Supporting Information). In a typical experiment, 25 mg of pristine GrNP was combined with 50 mL EtOAc (0.5 mg/mL) and 100 g of YSZ media in an 80-mL nylon jar, or 230 g of milling media in a 100-mL Pyrex glass bottle with a heavy-duty polypropylene cap. The contents were milled for 48 hours at room temperature, then transferred by glass syringe to a 100-mL beaker and cooled in an ice bath. The dispersion was sonicated for 1 hour at 180 W with an on/off duty cycle of 10 s

and 3 s (fluence = 4.98 kJ) using a 13-mm Ti immersion probe (FS-450N, Mxbaoheng), then centrifuged for 30 minutes at 4000 rpm using a swinging-bucket centrifuge (Thermo Scientific). The final dispersions were harvested from the upper two-thirds of the supernatant and stored in glass containers at room temperature. GrNP suspensions were deposited onto substrates using a mounted air-spray gun (Model G222, Master Airbrush) and performed under ambient conditions at a rate of approximately 1.5 mL/min and pressure of 25–30 psi, with a 0.5-mm needle emitter positioned 8 cm from the surface. Coating thickness and rms roughness (R_g) were determined by AFM linescans relative to a fiducial scratch mark.

Fabrication of solid-contact ion-selective electrodes and potentiometric analysis. GrNP dispersions were deposited onto square heads of carbon electrodes (6 × 6 mm^2) screen-printed on PET films using a spray time of 2 minutes, to produce a continuous layer with estimated thickness of 0.25 μm. Nitrate-selective membranes were deposited onto each electrode head by drop-casting 0.1 mL of a solution consisting of high molecular weight PVC (2.0 g), DBP (4.0 g), and TOAN (0.134 g) dissolved in THF (20 mL). After drying under ambient conditions for one day, the rest of the electrode was passivated with an adhesive silicone coating (Silicone Solutions, SS-6002S) and left to dry in air for at least one day prior to use. ISEs were immersed in 1 mM KNO_3 for one day before obtaining potentiometric readouts in aqueous solutions of KNO_3 from 10^{-4} M to 10^{-1} M. Electrodes were immersed in each nitrate solution for 2 minutes and rinsed with deionized water between measurements.

RESULTS AND DISCUSSION

Liquid-phase exfoliation (LPE) is one of the most widely used methods to generate dispersions of few-layer graphene.[39] However, most of these employ energy-intensive processes such as sonication at high power, high-shear mixing, or microfluidization.[8,9,13–15,19–21] Liquid-

assisted ball milling is also a form of LPE but requires much lower input energy, particularly if tumbling mills can be used. In this work we evaluate horizontal ball milling as a practical method of exfoliating graphene in aprotic organic solvents.

Characterization of Exfoliated Graphene Nanoplatelets. GrNPs in powder form were added to dry EtOAc or acetone in ball-milling jars and mixed on a tumbling mill for up to 48 hours at ambient temperatures, then subjected to sonication at moderate power for 1 hour at 0 °C followed by centrifugation and collection of the supernatant (see Experimental Section). These dispersions are stable for at least several months at ambient temperatures by visual inspection with less than 4% change over 7 weeks as monitored by optical extinction spectroscopy (Figure 1A). To obtain a standard curve for optical analysis, aliquots of the GrNP dispersion were collected onto Al_2O_3 membranes with 0.1-μm pores using pressure-driven filtration and weighed on an analytical balance, which yielded an extinction coefficient at 660 nm (ε_{660}) of 212.7 L g^{-1} m^{-1} for exfoliated GrNP in EtOAc (Figure 1B). This ε_{660} value is much lower than those reported for other graphene dispersions, which range between 700 and 6600 L g^{-1} m^{-1}.[19,40]

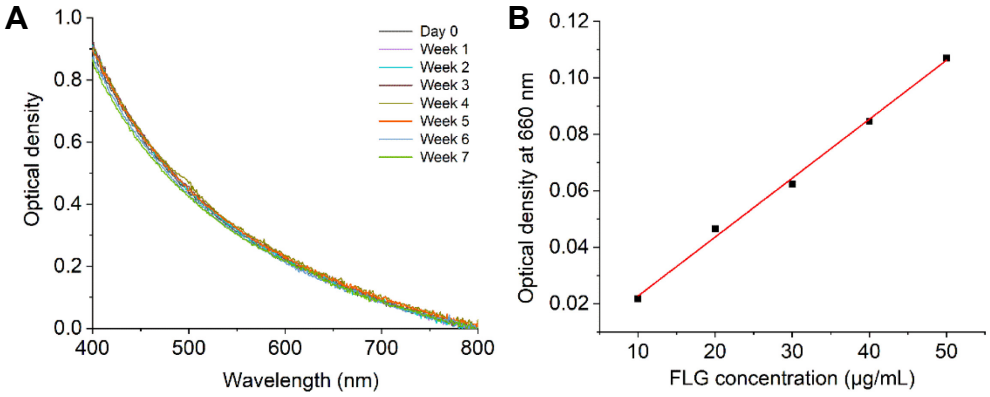

Figure 1. (A) Extinction spectra of GrNP dispersion in EtOAc over a 7-week period; (B) extinction coefficient in EtOAc (ε_{660} = 212.7 L g^{-1} m^{-1}).

It is worth noting that particle size and aggregation can contribute heavily to optical extinction through scattering, however the median size of exfoliated GrNP in our samples is 180 nm (see below) so its ε_{660} value is mostly due to absorption.

While low-energy ball milling is useful for liquid-assisted exfoliation, it is not sufficient to maintain stable dispersions of GrNPs in moderately polar solvents such as EtOAc, with apparent flocculation within 48 hours. Dispersion stability can be optimized by subjecting exfoliated GrNPs to sonication at 0 °C, with immersion probes providing higher efficiency and reproducibility than ultrasonic baths. Interestingly, we observe that GrNP concentration is adversely impacted at high sonication power: sonication at 450 W (1246 kJ fluence) generates less than half the amount of exfoliated GrNP produced at 180 W (498 kJ fluence; Figure 2). We attribute the loss in stability to aerobic oxidation of exfoliated graphene and subsequent aggregation in aprotic solvent.

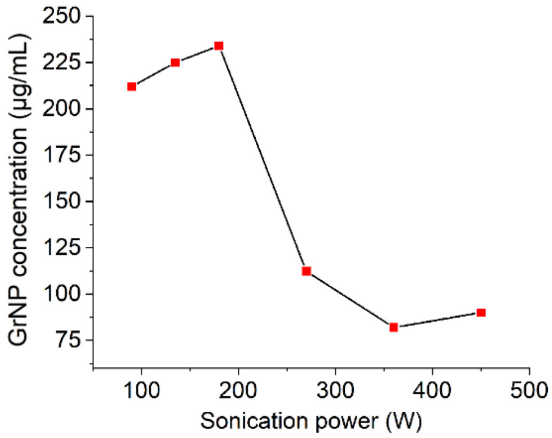

Figure 2. Concentrations of GrNPs dispersed in EtOAc as a function of sonication power; GrNPs were milled for 48 hours prior to sonication.

GrNPs milled for 48 hours in dry EtOAc and sonicated at moderate power (180 W) can produce a dispersion of 235 µg/mL from an initial loading of 0.5 mg/mL and 356 µg/mL from

1.0 mg/mL, corresponding to yields by weight (Y_W) of 47 and 36% respectively. Similarly, GrNPs milled for 48 hours in dry acetone can produce a dispersion of 310 μg/mL from an initial loading of 0.5 mg/mL for a Y_W of 62%. We note that GrNP concentration increases with milling time in roughly linear fashion (Figure S2), and thus believe these values to be far from the upper limit for stable GrNP dispersions. Coleman and co-workers previously reported stable graphene dispersions up to 25 mg/mL in NMP;[20] more recently, exfoliation studies involving circulating shear mixing and wet-jet milling generated surfactant-stabilized graphene dispersions of 100 mg/mL or more after many thousands of cycles, with Y_W approaching 100%.[41,42]

Solvent quality is an important but frequently overlooked factor in the production of colloidal dispersions at high concentration. The best GrNP dispersions are produced when using solvents in pristine condition: commercial sources of HPLC-grade EtOAc can be used if protected from air and moisture and consumed within several weeks, whereas reagent-grade acetone must be further dried over molecular sieves before use. To illustrate the effect of air exposure, we performed control experiments using a freshly opened bottle of EtOAc saturated with dry air from a purge-gas generator, and a bottle of EtOAc that had been opened multiple times over a 2-month period. GrNP dispersions prepared under identical conditions were clearly impacted by the source of EtOAc, with aerated and aged solvents containing 30% and 60% less GrNP respectively (Figure S3A, Supporting Information). It must also be noted that the GrNP source is important for efficient exfoliation (see Experimental Section); studies with an alternate source of GrNP and graphite powder produced dispersions of lower density (Figure S3B) with complete flocculation after two weeks, whereas the GrNP dispersions described in Figure 1 remain well dispersed for at least several months.

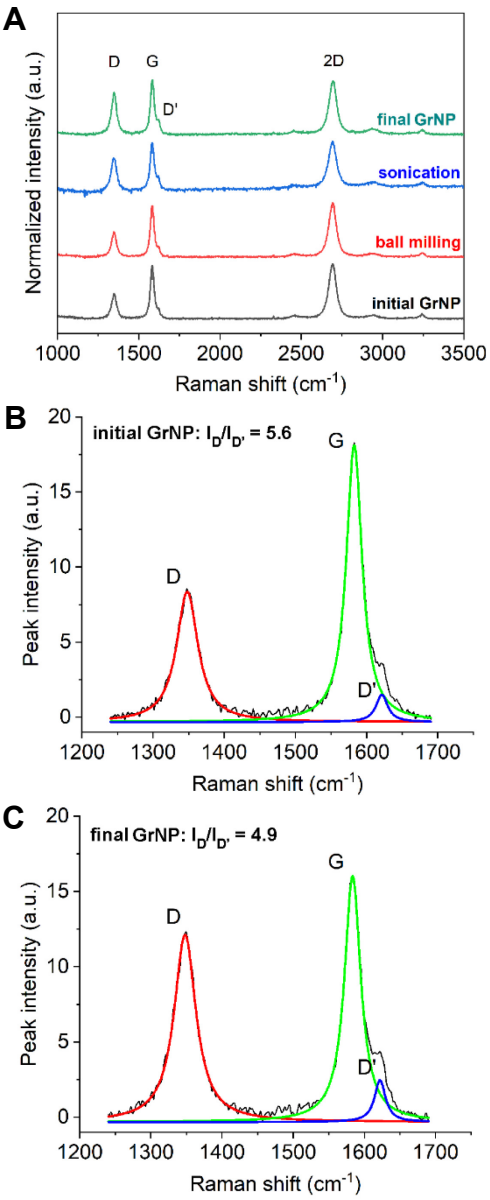

Figure 3. (A) Raman analysis of GrNPs during the exfoliation process. (B,C) An increase in D/G but not D/D' peak ratios suggests that structural changes to GrNPs during liquid-phase exfoliation are related primarily to particle size reduction.

Raman analysis of GrNPs at different stages of exfoliation showed a gradual increase in the ratio of D and G peak intensities (at 1350 and 1580 cm^{-1} respectively) from 0.46 to 0.75 (Figure 3). Although a high D/G ratio is often associated with increases in structural defects,[43,44] the peakwidth of the G bands for GrNPs before and after solution processing hardly changed

(FWHM of 29.53 cm^{-1} and 28.58 cm^{-1}, respectively) indicating no increase in structural disorder.[43] Furthermore, peak deconvolution reveals that the ratio of D and D' peak intensities ($I_D/I_{D'}$) did not increase (5.6 for pristine GrNPs versus 4.9 for the final dispersion), the latter being associated with increased structural disorder.[45] The $I_D/I_{D'}$ ratios indicate that changes in graphene structure generated during LPE are mainly related to a reduction in particle size, rather than oxidation or vacancy defects: a low ratio correlates with domain boundary defects along the lattice edges, whereas $I_D/I_{D'}$ ratios above 7 correlate with vacancies or sp^3-type defects in the graphene lattice.[44] It is worth mentioning that ATR-IR analysis was performed on GrNPs in pristine form, after liquid-assisted ball milling, and after moderate sonication, but no additional peaks in the regions corresponding to C=O or C=C–O stretching (generated by carboxyl or phenolic groups) were detected (data not shown).

It is worth mentioning that ball milling should be performed with yttrium-stabilized zirconia (YSZ) media, even when using low-impact tumbling mills. XPS analysis of ball-milled graphene using zirconia media reveals a doublet in the Zr 3d region, characteristic of ZrO_2 (Figure S4A, Supporting Information). Scanning transmission electron microscopy (STEM) with energy dispersive X-ray spectroscopic (EDS) imaging confirmed Zr contamination in ZrO_2-milled graphene, whereas GrNPs exfoliated with YSZ milling media was free of residual Zr (Figure S4B–E). All studies in this work were performed with GrNPs exfoliated by YSZ media.

Structural analysis of individual GrNP particles confirmed most of these to be few-layered graphene. Nanoflakes were characterized by atomic force microscopy (AFM) by depositing a diluted EtOAc dispersion of GrNPs using an airspray brush onto Si/SiO_2 substrate (Figure 4A); the median height and lateral width was 4.1 nm and 180 nm, respectively (Figure 4B,C). In comparison, our commercial source of GrNPs (produced by thermal plasma treatment

of methane) are reported to have a mean thickness of 2.4 nm and lateral size of 150–200 nm, prior to their collection in powder form.[38] The mean height of the thinnest particles was 1.35 ± 0.05 nm and corresponds with bilayer graphene, in accord with earlier AFM analyses of exfoliated graphene on Si/SiO_2.[46,47] This was confirmed by selected area electron diffraction (SAED) of a TEM image, which clearly revealed hexagonal patterns characteristic of the {1100} and {2110} lattice planes of bilayer graphene (Figure 4D,E).[13] The median GrNP particle has 8–10 layers of graphene, based on increases in thickness of ~0.35 nm for each additional layer.

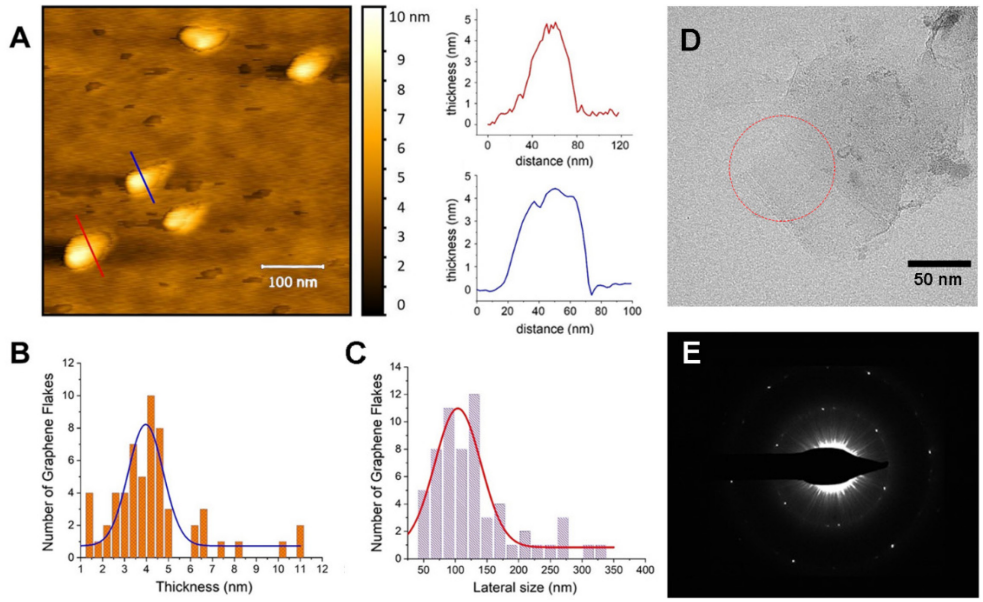

Figure 4. (A–C) AFM analysis of individual GrNPs exfoliated in EtOAc. (A) Representative image of individual particles with linescans; (B) distribution of particle heights (0.35-nm bin width, *N*=61); (C) distribution of lateral cross sections (20-nm bin width; *N*=58). (D,E) TEM image and SAED pattern of bilayer graphene particle (taken from dashed circle).

Spray-coating of Graphene Nanoplatelet Dispersions. A primary benefit of dispersing graphene and other nanomaterials in volatile organic solvents is the ease with which they can be

deposited by various spray-coating methods. Ethyl acetate is a popular medium for spray technologies because of its rapid drying rate with low residue,[48,49,50] in addition to its favorable profile as a safe and sustainable solvent (Table 1). In the examples below, a standard air-spray gun was used to deposit GrNP dispersions onto Si/SiO_2 (electrically conductive films), screen-printed carbon electrodes on polyethylene terephthalate (PET) (potentiometric sensors), and metal heat sinks for enhancing their rates of heat dissipation.

GrNP dispersions in ethyl acetate (235 μg/mL) were spray-coated at a rate of 1.5 mL/min and at ambient temperature onto freshly cleaned Si/SiO_2 substrates, which were dry to the touch within seconds and with no detectable solvent vapor after 1 min. The graphene coating thickness was fairly uniform but did not increase linearly with deposition time; for example, spraying 3 mL of GrNP dispersion produced a mean thickness (t_{av}) of 220 nm with a rms roughness (R_q) of 31 nm, whereas spraying 12 mL produced t_{av} and R_q of 500 and 63 nm, respectively (Figure S5 and Table S1, Supporting Information). To characterize their electrical conductivity, four-probe Au electrodes were deposited thermally onto GrNP-coated substrates through a pre-patterned shadow mask (Figure 5). Sheet resistance scales in proportion to the density of interparticle contacts, so the spray-coated GrNP films are expected to be less conductive than those prepared by the transfer of large-area graphene.[15] However, the spray-coated films proved to be remarkably conductive despite the small lateral size of GrNPs: a 220-nm layer exhibited a mean sheet resistance (R_S) of 5.5 kΩ/sq. and estimated conductivity (σ) of 8.3 S/cm, whereas a 500-nm layer had mean Rs and σ values of 1.1 kΩ/sq. and 18.9 S/cm, respectively. A recent study by Barz and coworkers reported conductivities up to 45 S/cm for GrNPs mixed with 10% reduced graphene oxide (rGO).[51] Films were prepared by dispensing aqueous dispersions of GrNPs (15 mg/mL) and 10% GO (1.5 mg/mL), followed by treatment with ascorbic acid and two rounds of

oven drying (1 hour each). In comparison, films prepared by the spray coating of dilute GrNP dispersions in EtOAc were fully dried in under one minute at room temperature and were characterized without further treatment.

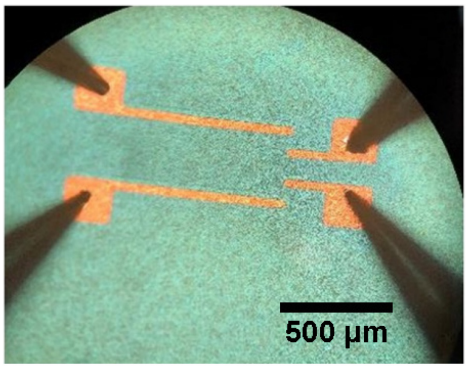

Figure 5. Four-point probe analysis of spray-coated GrNP film on Si/SiO_2.

Applications of Spray-coated Graphene Nanoplatelets. Conductive nanocarbons with high surface area can support EDLs at high charge densities. For example, when graphene is deposited as a solid contact between an ionically conductive membrane and an electrically conductive electrode, changes in ion concentration at the membrane–contact interface are relayed into shifts in phase boundary potential at the contact–electrode interface in accord with the Nernst equation.[52] EDL-based solid contacts for ion-selective electrodes may also provide additional benefits such as the normalization of potentiometric readouts and stabilization against voltage drift during measurements.[53,58,59] We recently demonstrated that depositing GrNP contact layers onto screen-printed carbon substrates helped to preserve their performance as pH electrodes over multiple weeks.[54] In this work we show that spray-coated GrNP films substantially improves the intrabatch reproducibility of solid-state ISEs developed for low-cost nitrate sensing.

A continuous GrNP layer (~0.25 µm thickness) was spray-coated onto the heads of screen-printed carbon electrodes (*N*=8) followed by deposition of a nitrate-selective membrane; a set of control electrodes without GrNP interfaces was also prepared (see Experimental Section). Both types of electrodes provided a nearly Nernstian response to changes in nitrate concentration between 0.1 and 100 mM (54 mV/dec sensitivity); however, the range of voltage readouts for electrodes with graphene solid contacts was considerably narrower (Figure 6). Electromotive force (EMF) values for electrodes with GrNP-based contacts fell within a 10-mV window, whereas those without solid contacts exhibited a wider spread of 23 mV. The tighter distribution of EMF values has important ramifications for using cost-effective manufacturing processes to produce high-quality sensors at low cost. The production of disposable ISEs can be scaled up using roll-to-roll manufacturing methods;[55] in this regard, we have determined the feasibility of depositing GrNP dispersions onto roll substrates by in-line spray coating, prior to membrane casting (Figure S6, Supporting Information).

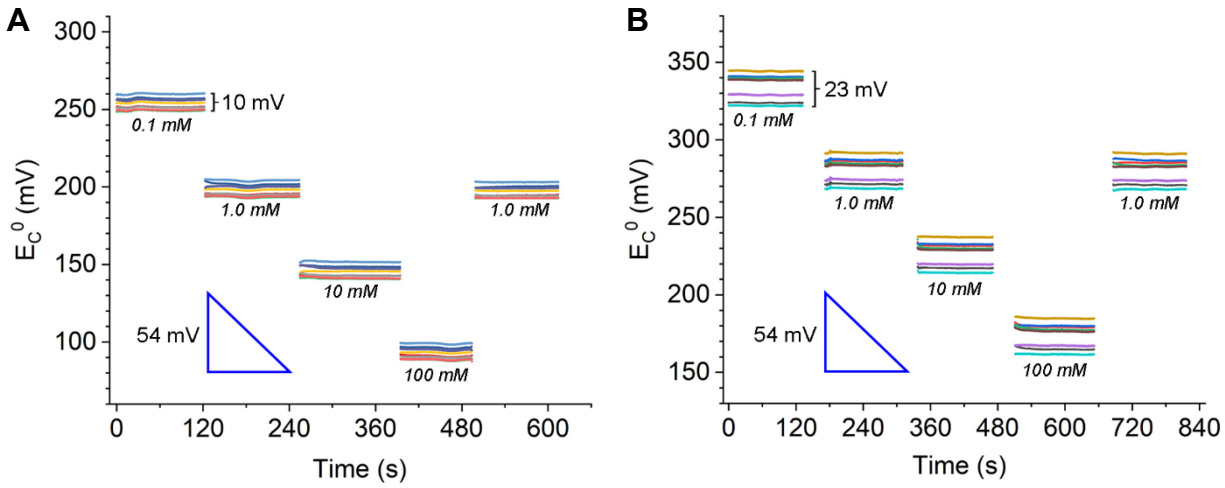

Figure 6. Spray-coated GrNP contact improves the intrabatch reproducibility of solid-state electrodes for potentiometry. (A) Nitrate-sensing electrodes with graphene contact layers exhibit a voltage spread of 10 mV (*N*=8); (B) electrodes without GrNP-based contacts have a spread of 23 mV (*N*=8).

Graphite is also well known for its excellent thermal conductivity, and graphene-based dispersions and composites have been widely studied as media for heat dissipation and exchange.[33–35,56,57] To determine whether the high surface area of GrNPs could be used to increase the rate of radiative heat transfer, dispersions of GrNPs were spray-coated onto the fins of aluminum heat sinks mounted on the backs of thermoelectric Peltier blocks (see Experimental Section). The plates generated substantial amounts of heat when powered by a 12-V/5-Ah battery, with heat sink fins achieving a steady-state temperature of nearly 80 °C in ambient conditions (22.8 °C). Changes in surface temperatures after cutting electrical power were recorded by a thermal imaging camera (Figure 7A), with the largest drops observed during the first few seconds. Heat sink fins coated with a 0.5-μm layer of GrNP had a quasi-linear cooling rate of 0.63 °C/s during the first 15 seconds, which was 20% faster than uncoated heat sink fins (0.52 °C/s; Figure 7B). This result is line with other examples of graphene-based materials for heat dissipation: the thermal conductivity of an all-graphene heat sink was reported to be several times greater than its metal counterparts,[56] and a heat sink fashioned from porous copper–reduced graphene oxide (rGO) maintained lower temperatures relative to one without rGO.[57]

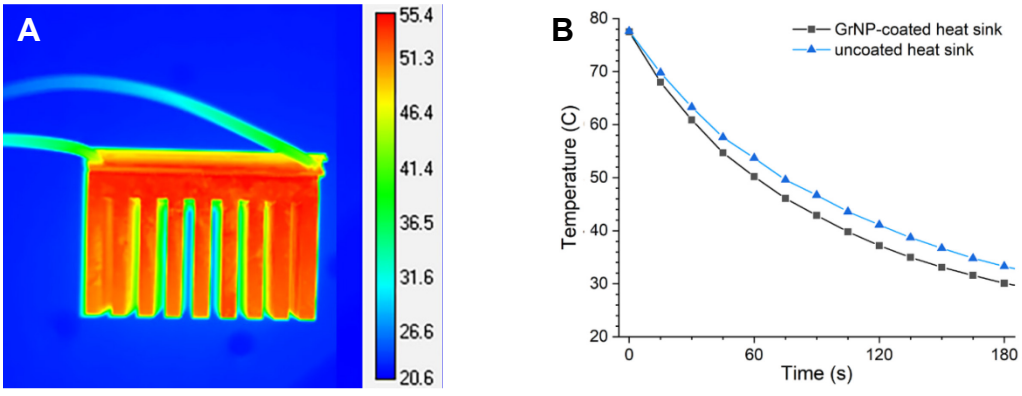

Figure 7. Heat dissipation from GrNP-coated heat sink. (A) Thermal imaging of heat sink mounted on back side of Peltier plate while cooling; (B) thermal decay from heat sink fins after cutting electrical power.

CONCLUSIONS

Stable dispersions of graphene nanoplatelets in volatile, high-PEL solvents such as ethyl acetate and acetone are ideal for manufacturing processes that benefit from rapid deposition and drying. The use of low-energy ball milling for liquid-assisted exfoliation and spray coating for thin-film deposition can support sustainable device manufacturing, starting with GrNPs or other 2D materials in commercial powder forms. GrNP dispersions in volatile organic solvents can be generated on even larger scales and higher concentrations using continuous high-shear mixing or microfluidization, if appropriate attention is paid toward solvent quality. The methods reported here can be performed at ambient conditions and pressures and are compatible with in-line processes for additive manufacturing, as illustrated by the deposition of GrNPs as solid contacts for thin-film potentiometric sensors with reproducible intrabatch performance, and the coating of heat sinks for increased dissipation of thermal energy.

SUPPORTING INFORMATION

Equipment and additional data for liquid-assisted exfoliation and scalable manufacturing; XPS and AFM analytical data.

ACKNOWLEDGMENTS

We gratefully acknowledge financial and technical support from the SMART Films consortium and the Birck Nanotechnology Center at Purdue University, The National Science Foundation (CHE-2204206, DMR-2016453), the Office of Naval Research (N00014-22-1-2127), the Air Force Research Laboratory (SEMI-FlexTech-NBMC Project # NB18-21-27), Robert Nicholas

for assistance with ATR-IR measurements, and discussions with Nick Glassmaker, James Lallo, and Jianguo Mei.

REFERENCES

[1] Novoselov, K. S.; Geim, A. K.; Morozov, S. V.; Jiang, D.; Zhang, Y.; Dubonos, S. V.; Grigorieva, I. V.; Firsov, A. A. Electric Field Effect in Atomically Thin Carbon Films. *Science* **2004**, *306*, 666-669.

[2] Edwards, R. S.; Coleman, K. S. Graphene synthesis: relationship to applications. *Nanoscale* **2013,** *5*, 38-51.

[3] Partoens, B.; Peeters, F. M. From graphene to graphite: Electronic structure around the *K* point. *Phys. Rev. B* **2006**, *74*, 075404.

[4] Torrisi, F.; Hasan, T.; Wu, W.; Sun, Z.; Lombardo, A.; Kulmala, T. S.; Hsieh, G.-W.; Jung, S.; Bonaccorso, F.; Paul, P. J.; Chu, D.; Ferrari, A. C. Inkjet-Printed Graphene Electronics. *ACS Nano* **2012**, *6*, 2992-3006.

[5] Stoller, M. D.; Park, S.; Zhu, Y.; An, J.; Ruoff, R. S. Graphene-Based Ultracapacitors. *Nano Lett.* **2008**, *8*, 3498-3502.

[6] Gao, L.; Ni, G.-X.; Liu, Y.; Liu, B.; Castro Neto, A. H.; Loh, K. P. Face-to-face transfer of wafer-scale graphene films. *Nature* **2014**, *505*, 190-194.

[7] Lee, J. S.; Joung, H.-A.; Kim, M.-G.; Park, C. B. Graphene-Based Chemiluminescence Resonance Energy Transfer for Homogeneous Immunoassay. *ACS Nano* **2012**, *6*, 2978-2983.

[8] Yi, M.; Shen, Z. A review on mechanical exfoliation for the scalable production of graphene. *J. Mater. Chem. A* **2015**, *3*, 11700-11715.

[9] Johnson, D. W.; Dobson, B. P.; Coleman, K. S., A manufacturing perspective on graphene dispersions. *Curr. Op. Colloid Interface Sci.* **2015,** *20*, 367-382.

[10] Kesarwani, S.; Verma, R. K., A Critical Review on Synthesis, Characterization and Multifunctional Applications of Reduced Graphene Oxide (rGO)/Composites. *Nano* **2021,** *16*, 2130008.

[11] Kumar, N.; Salehiyan, R.; Chauke, V.; Joseph Botlhoko, O.; Setshedi, K.; Scriba, M.; Masukume, M.; Sinha Ray, S. Top-down synthesis of graphene: A comprehensive review. *FlatChem* **2021,** *27*, 100224.

[12] Abdelkader, A.; Cooper, A.; Dryfe, R. A.; Kinloch, I. How to get between the sheets: a review of recent works on the electrochemical exfoliation of graphene materials from bulk graphite. *Nanoscale* **2015,** *7*, 6944-6956.

[13] Lotya, M.; Hernandez, Y.; King, P. J.; Smith, R. J.; Nicolosi, V.; Karlsson, L. S.; Blighe, F. M.; De, S.; Wang, Z.; McGovern, I. T.; Duesberg, G. S.; Coleman, J. N. Liquid Phase Production of Graphene by Exfoliation of Graphite in Surfactant/Water Solutions. *J. Am. Chem. Soc.* **2009**, *131*, 3611-3620.

[14] Guardia, L.; Fernández-Merino, M. J.; Paredes, J. I.; Solís-Fernández, P.; Villar-Rodil, S.; Martínez-Alonso, A.; Tascón, J. M. D. High-throughput production of pristine graphene in an aqueous dispersion assisted by non-ionic surfactants. *Carbon* **2011**, *49*, 1653-1662.

[15] Lotya, M.; King, P. J.; Khan, U.; De, S.; Coleman, J. N. High-Concentration, Surfactant-Stabilized Graphene Dispersions. *ACS Nano* **2010**, *4*, 3155-3162.

[16] Sethurajaperumal, A.; Varrla, E. High-Quality and Efficient Liquid-Phase Exfoliation of Few-Layered Graphene by Natural Surfactant. *ACS Sustain. Chem. Eng.* **2022**. DOI: 10.1021/acssuschemeng.2c03742.

[17] Fernández-Merino, M. J.; Paredes, J. I.; Villar-Rodil, S.; Guardia, L.; Solís-Fernández, P.; Salinas-Torres, D.; Cazorla-Amorós, D.; Morallón, E.; Martínez-Alonso, A.; Tascón, J. M. D., Investigating the influence of surfactants on the stabilization of aqueous reduced graphene oxide dispersions and the characteristics of their composite films. *Carbon* **2012,** *50*, 3184-3194.

[18] Irin, F.; Hansen, M. J.; Bari, R.; Parviz, D.; Metzler, S. D.; Bhattacharia, S. K.; Green, M. J., Adsorption and removal of graphene dispersants. *J. Colloid Interface Sci.* **2015,** *446*, 282-289.

[19] Coleman, J. N. Liquid Exfoliation of Defect-Free Graphene. *Acc. Chem. Res.* **2013**, *46*, 14-22.

[20] Khan, U.; Porwal, H.; O'Neill, A.; Nawaz, K.; May, P.; Coleman, J. N. Solvent-Exfoliated Graphene at Extremely High Concentration. *Langmuir* **2011**, *27*, 9077-9082.

[21] Barwich, S.; Khan, U.; Coleman, J. N. A Technique to Pretreat Graphite Which Allows the Rapid Dispersion of Defect-Free Graphene in Solvents at High Concentration. *J. Phys. Chem. C* **2013**, *117*, 19212-19218.

[22] Department of Industrial Relations, California Code of Regulations, Title 8, Section 5155, Table AC-1. https://www.dir.ca.gov/title8/5155table_ac1.html (accessed June 16. 2022)

[23] NIOSH Pocket Guide to Chemical Hazards. National Institute for Occupational Safety and Health, Centers for Disease Control and Prevention: Washington, DC, 2020. https://www.cdc.gov/niosh/npg/default.html (accessed June 16, 2022)

[24] Capello, C.; Fischer, U.; Hungerbühler, K. What is a green solvent? A comprehensive framework for the environmental assessment of solvents. *Green Chem.* **2007**, *9*, 927-934.

[25] Byrne, F. P.; Jin, S.; Paggiola, G.; Petchey, T. H. M.; Clark, J. H.; Farmer, T. J.; Hunt, A. J.; Robert McElroy, C.; Sherwood, J., Tools and techniques for solvent selection: Green Solvent Selection Guides. *Sustain. Chem. Process.* **2016,** *4*, 7.

[26] Prat, D.; Hayler, J.; Wells, A., A Survey of Solvent Selection Guides. *Green Chem.* **2014,** *16*, 4546-4551.

[27] ECHA Candidate List of Substances of Very High Concern for Authorisation. https://echa.europa.eu/candidate-list-table (accessed June 16, 2022)

[28] Final Scope of the Risk Evaluation for *o*-Dichlorobenzene. U.S. Environmental Protection Agency, Document EPA-740-R-20-001, August 2020.

[29] Hernandez, Y.; Lotya, M.; Rickard, D.; Bergin, S. D.; Coleman, J. N., Measurement of Multicomponent Solubility Parameters for Graphene Facilitates Solvent Discovery. *Langmuir* **2010,** *26*, 3208-3213.

[30] O'Neill, A.; Khan, U.; Nirmalraj, P. N.; Boland, J.; Coleman, J. N. Graphene Dispersion and Exfoliation in Low Boiling Point Solvents. *J. Phys. Chem. C* **2011**, *115*, 5422-5428.

[31] Garakani, M. A.; Bellani, S.; Pellegrini, V.; Oropesa-Nuñez, R.; Castillo, A. E. D. R.; Abouali, S.; Najafi, L.; Martín-García, B.; Ansaldo, A.; Bondavalli, P.; Demirci, C.; Romano, V.; Mantero, E.; Marasco, L.; Prato, M.; Bracciale, G.; Bonaccorso, F., Scalable spray-coated graphene-based electrodes for high-power electrochemical double-layer capacitors operating over a wide range of temperature. *Energ. Stor. Mater.* **2021,** *34*, 1-11.

[32] Sun, Q.; Li, W.; Su, B., Highly hydrophobic solid contact based on graphene-hybrid nanocomposites for all solid state potentiometric sensors with well-formulated phase boundary potentials. *J. Electroanal. Chem.* **2015,** *740*, 21-27.

[33] Natesan, K.; Karinka, S., A comprehensive review of heat transfer enhancement of heat exchanger, heat pipe and electronic components using graphene. *Case Stud. Therm. Eng.* **2023,** *45*, 102874.

[34] Kim, S. Y.; Noh, Y. J.; Yu, J., Thermal conductivity of graphene nanoplatelets filled composites fabricated by solvent-free processing for the excellent filler dispersion and a theoretical approach for the composites containing the geometrized fillers. *Compos. Part A Appl. Sci. Manuf.* **2015,** *69*, 219-225.

[35] Agromayor, R.; Cabaleiro, D.; Pardinas, A. A.; Vallejo, J. P.; Fernandez-Seara, J.; Lugo, L., Heat Transfer Performance of Functionalized Graphene Nanoplatelet Aqueous Nanofluids. *Materials* **2016,** *9*, 455.

[36] Prat, D.; Wells, A.; Hayler, J.; Sneddon, H.; McElroy, C. R.; Abou-Shehada, S.; Dunn, P. J. CHEM21 selection guide of classical- and less classical-solvents. *Green Chem.* **2016**, *18*, 288-296.

[37] Colley, S.W.; Fawcett, C.R.; Rathmell, C.; Tuck, M.W.M. Process for the Preparation of Ethyl Acetate. US Patent 6,809,217, 2004.

[38] (a) Kroeger, J.; Larouche, N.; Larouche, F. Plasma Processes for Producing Graphene Nanosheets. US Patent 10,843,925, 2020. (b) https://nanointegris.com/our-products/graphene-purewave-nanoplatelets-powder (last accessed 06/22/2023).

[39] Xu, Y.; Cao, H.; Xue, Y.; Li, B.; Cai, W., Liquid-Phase Exfoliation of Graphene: An Overview on Exfoliation Media, Techniques, and Challenges. *Nanomaterials* **2018,** *8*, 942.

[40] Ojrzynska, M.; Wroblewska, A.; Judek, J.; Malolepszy, A.; Duzynska, A.; Zdrojek, M. Study of optical properties of graphene flakes and its derivatives in aqueous solutions. *Opt. Express* **2020,** *28*, 7274-7281.

[41] Carey, T.; Alhourani, A.; Tian, R.; Seyedin, S.; Arbab, A.; Maughan, J.; Šiller, L.; Horvath, D.; Kelly, A.; Kaur, H.; Caffrey, E.; Kim, J. M.; Hagland, H. R.; Coleman, J. N., Cyclic production of biocompatible few-layer graphene ink with in-line shear-mixing for inkjet-printed electrodes and Li-ion energy storage. *npj 2D Mater. Appl.* **2022,** *6*, 3.

[42] Del Rio Castillo, A. E.; Pellegrini, V.; Ansaldo, A.; Ricciardella, F.; Sun, H.; Marasco, L.; Buha, J.; Dang, Z.; Gagliani, L.; Lago, E.; Curreli, N.; Gentiluomo, S.; Palazon, F.; Prato, M.; Oropesa-Nuñez, R.; Toth, P. S.; Mantero, E.; Crugliano, M.; Gamucci, A.; Tomadin, A.; Polini, M.; Bonaccorso, F., High-yield production of 2D crystals by wet-jet milling. *Mater. Horiz.* **2018,** *5*, 890-904.

[43] Cançado, L. G.; Jorio, A.; Ferreira, E. H. M.; Stavale, F.; Achete, C. A.; Capaz, R. B.; Moutinho, M. V. O.; Lombardo, A.; Kulmala, T. S.; Ferrari, A. C., Quantifying Defects in Graphene via Raman Spectroscopy at Different Excitation Energies. *Nano Lett.* **2011,** *11*, 3190-3196.

[44] Eckmann, A.; Felten, A.; Mishchenko, A.; Britnell, L.; Krupke, R.; Novoselov, K. S.; Casiraghi, C., Probing the nature of defects in graphene by Raman spectroscopy. *Nano Lett.* **2012,** *12*, 3925-3930.

[45] Childres, I.; Jauregui, L. A.; Park, W.; Cao, H.; Chen, Y. P., Raman Spectroscopy of Graphene and Related Materials. In *New Developments in Photon and Materials Research*, Jang, J. I., Ed. Nova Publishers: 2013; pp 403–418.

[46] Novoselov, K. S.; Jiang, D.; Schedin, F.; Booth, T. J.; Khotkevich, V. V.; Morozov, S. V.; Geim, A. K., Two-dimensional atomic crystals. *Proc. Natl. Acad. Sci.* **2005,** *102*, 10451-10453.

[47] Vallés, C.; Drummond, C.; Saadaoui, H.; Furtado, C. A.; He, M.; Roubeau, O.; Ortolani, L.; Monthioux, M.; Pénicaud, A., Solutions of Negatively Charged Graphene Sheets and Ribbons. *J. Am. Chem. Soc.* **2008,** *130*, 15802-15804.

[48] Wang, F.J.; Wang, C.H., Sustained release of etanidazole from spray dried microspheres prepared by non-halogenated solvents. *J Control Release* **2002**, *81*, 263-280.

[49] Kauppinen, A.; Broekhuis, J.; Grasmeijer, N.; Tonnis, W.; Ketolainen, J.; Frijlink, H. W.; Hinrichs, W. L. J., Efficient production of solid dispersions by spray drying solutions of high solid content using a 3-fluid nozzle. *Eur. J. Pharm. Biopharm.* **2018,** *123*, 50-58.

[50] Hou, C.; Liu, M.; Xu, C.; Ma, J., Preparation and characterization of CL-20/NTO/Estane5703 composite microspheres by spray drying. *AIP Adv.* **2022,** *12*, 035049.

[51] Mypati, S.; Sellathurai, A.; Kontopoulou, M.; Docoslis, A.; Barz, D. P. J., High concentration graphene nanoplatelet dispersions in water stabilized by graphene oxide. *Carbon* **2021,** *174*, 581-593.

[52] Hu, J.; Stein, A.; Bühlmann, P., Rational design of all-solid-state ion-selective electrodes and reference electrodes. *Trends Anal. Chem* **2016,** *76*, 102-114.

[53] Hu, J.; Ho, K. T.; Zou, X. U.; Smyrl, W. H.; Stein, A.; Bühlmann, P., All-Solid-State Reference Electrodes Based on Colloid-Imprinted Mesoporous Carbon and Their Application in Disposable Paper-based Potentiometric Sensing Devices. *Anal. Chem.* **2015,** *87*, 2981-2987.

[54] Yermembetova, A.; Oduncu, M. R.; Wei, A., Radiation-tolerant thin-film electrodes for pH monitoring in sterile media. *Anal. Chem.* **2022,** *94*, 15535–15540.

[55] Glassmaker, N. J.; Mi, Y.; Cakmak, M.; Shakouri, A., Roll-to-roll manufacturing, in-line imaging, and characterization of functional films. *Proc. ASME 17th Int. Manuf. Sci. Eng. Conf.* **2022**, 85553.

[56] Wang, N.; Liu, Y.; Ye, L.; Li, J. In *Highly Thermal Conductive and Light-weight Graphene-based Heatsink*, 2019 22nd European Microelectronics and Packaging Conference & Exhibition (EMPC), 16-19 Sept. 2019; 2019; pp 1-4.

[57] Rho, H.; Jang, Y. S.; Bae, H.; Cha, A.-N.; Lee, S. H.; Ha, J.-S., Fanless, porous graphene-copper composite heat sink for micro devices. *Sci. Rep.* **2021,** *11*, 17607.

[58] Ulloa, A. M.; Glassmaker, N. J.; Oduncu, M. R.; Xu, P.; Wei, A.; Cakmak, M.; Stanciu, L. Roll-to-Roll Manufactured Sensors for Nitroaromatic Organophosphorus Pesticides Detection. *ACS Appl. Mater. Interfaces* **2021**, *13*, 35961-35971.

[59] Jin, X.; Saha, A.; Jiang, H.; Oduncu, M. R.; Yang, Q.; Sedaghat, S.; Maize, K. D.; Allebach, J. P.; Shakouri, A.; Glassmaker, N.; et al. Steady-State and Transient Performance of Ion-Sensitive Electrodes Suitable for Wearable and Implantable Electro-chemical Sensing. *IEEE Trans. Biomed. Eng.* **2022**, *69*, 96-107.

SYNOPSIS & GRAPHICAL ABSTRACT

Graphene nanoplatelets can be exfoliated efficiently in ethyl acetate or acetone, green solvents with moderate volatility and low toxicity, enabling their spray deposition onto heat sinks and as solid contacts for low-cost potentiometric ion sensors.